Granular Scaling Approach to Landslide Runout

Rory T Cerbus, Ludovic Brivady, Thierry Faug, Hamid Kellay

Granular Scaling Approach to Landslide Runout

Rory T. Cerbus,[1,2,*] Ludovic Brivady,[2] Thierry Faug,[3] and Hamid Kellay[2]
[1]RIKEN Center for Biosystems Dynamics Research (BDR), 2-2-3 Minatojima-minamimachi, Chuo-ku, Kobe 650-0047, Japan
[2]Laboratoire Ondes et Matière d'Aquitaine (LOMA), UMR 5798 Université Bordeaux et CNRS, 351 cours de la Libération, 33405 Talence, France
[3]Univ. Grenoble Alpes, CNRS, INRAE, IRD, Grenoble INP, IGE, 38000 Grenoble, France

(Received 16 February 2022; revised 17 January 2024; accepted 2 May 2024; published 20 June 2024)

A main objective in landslide research is to predict how far they will travel. Landslides are complex, and a complete understanding in principle requires accounting for numerous parameters. Here we engender a simplification by investigating the maximum landslide runout using granular laboratory experiments and a scaling analysis. We find that correctly accounting for the fall height and grain size distribution not only yields an improved correlation of normalized runout, but also quantitatively unites laboratory and field data. In particular, we find that the mobility of landslides increases with the square root of the fall height and with the skewness of the grain size distribution.

DOI: 10.1103/PhysRevLett.132.254101

The feature of landslides and avalanches of principal interest to the inhabitants of mountainous regions is how far they will reach. The cost in life and property in affected areas is enormous [1,2], with ecological hazards sometimes remaining decades later [3]. Predicting the runout distance, and in particular what parameters control it, is thus a major objective of landslide and avalanche research [4]. The variety and complexity of these parameters has encouraged a varied approach to this problem, and landslides and avalanches with different features are often treated as distinct. Highlighting the importance of features such as the slide geometry or soil content, landslides are commonly subdivided into nearly 30 different categories including debris flows and rock avalanches [5]. Snow avalanches are likewise treated as an entirely separate species of large mass movement [6]. A confounding problem is the difficulty to isolate and systematically study important parameters in nature. While laboratory experiments using small grains can methodically study features such as longitudinal ridges [7], the role of interstitial fluids [8,9], the overrun of dams [10], the generation of tsunamis [11], or the onset of avalanche behavior [12], these small-scale experiments are often argued to have only limited relevance to large-scale natural landslides and avalanches because of their vastly different time and length scales [13–15]. Thus the prevailing consensus, albeit not universal [16], is that while laboratory granular flows, snow avalanches, debris flows, and rock avalanches all share common features, their runout cannot be comprehended using a single approach.

Although an uncomplicated description of landslide runout appears to be out of the question, simple trends have been known for decades [4]. A classical result common among all natural systems is that the runout distance increases if the landslide is larger or falls from a greater height [4,15–17], although the exact dependence is not known. (For the sake of brevity we will hereafter refer to all natural and laboratory mass movements collectively as "landslides," regardless of their specific, intricate details.) This correlation between runout distance L, fall height H, and landslide volume V is typically demonstrated through plots of H/L versus V, where the nondimensional ratio $\mu = H/L$ is sometimes termed the effective friction or Heim's ratio [18]. Although the scatter in these plots can be substantial [4], it is generally agreed that as V increases, H/L decreases. Such plots thus demonstrate the possibility of uncovering a profound simplification in an otherwise impossibly complicated system, even if this is widely considered an incomplete description of landslide behavior [4,14,16,17].

The present work builds on the classical result represented by traditional plots of H/L versus V, and improves on it by determining how H is incorporated and by accounting for the granularity through the size distribution of the grain diameter D. The extreme scale separation between the grain size (typically ranging from $\sim 10^{-3}$ m to $\sim 10^{0}$ m; see Supplemental Material (SM) [19]) and either H ($\sim 10^{2}$ m) or L ($\sim 10^{3}$ m) suggests it is a negligible parameter, an implicit assumption in many continuum approaches. And yet it is an integral parameter in prominent granular rheologies [43,44], in understanding laboratory granular experiments [45], and in improving rheological models to replicate landslides [46]. Grain size has been used implicitly in rheologies that predict basal (bottom) friction [47], and explicitly in studies of air drag [48], but its influence on runout has only rarely been studied systematically [49], often being ignored altogether [16,17] or even declared irrelevant [14].

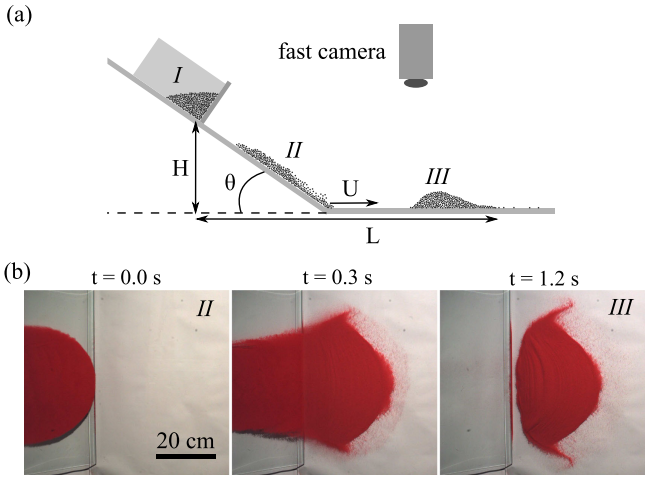

FIG. 1. (a) Side-view schematic of the experimental setup with (b) overhead images at intermediate (*II*) and final (*III*) times of the motion of $M \simeq 1300$ g of artificially colored red sand ($\langle D \rangle \simeq 250$ μm). The grains are released from a rectangular box (*I*) of width 15 cm via a sliding sluice gate at the front and slide down a flat glass plate (80 cm long and 65 cm wide), inclined at an angle $\theta \simeq 34°$, and eventually reach the junction (*II*) before coming to rest on a level flat glass plate (125×125 cm^2). The grain motion is observed with an overhead fast camera to determine the front speed U just after the junction. We use the frontmost position of the main mass to determine the runout L in our experiments.

Here, by explicitly and systematically accounting for D and H, we not only improve the correlation between L, H, and landslide size, but also weaken the boundaries between heretofore distinct flows. The implications of this result are twofold. First, the underlying physical mechanisms that control laboratory granular landslides and a number of natural landslides are apparently the same, potentially eliminating the need for emergent mechanisms to explain the runout of some large-scale landslides [14,50]. Second, laboratory-scale experiments can thus be fruitfully used to systematically investigate the quantitative behavior of even large-scale landslides, despite a widespread view to the contrary [13,15]. Our simple experiments and analysis thus serve to both unite disparate fields and potentially enlarge others [51].

We begin with laboratory experiments for which we systematically vary the fall height, the landslide size, and the grain size. The experimental setup is a simplified version of a natural landslide consisting of a slope, a flat section, grains, and a container to house the grains before releasing them by rapidly raising a sliding metal gate. See Fig. 1(a) for a schematic of the experimental setup. Natural landslides vary widely in the details of their initial conditions, and we make no attempt to replicate the specific features of any particular landslide geometry. While these details can affect some aspects of landslide dynamics, the runout distance itself is relatively insensitive [52]. In contrast to some previous studies [16], we define both H and L with reference to the front position for both the beginning and end of the landslide event.

For each experiment we measure the total mass M with a simple scale and gently sprinkle the grains into the rectangular box so that the surface is level. We then measure the total volume V of the initial grain pile using a standard measuring tape, which we also use to measure H and L. Because individual grains can escape and travel farther than the bulk, we identify the final front position as the frontmost position where a layer of grains is still in contact with the main mass [see Fig. 1(b)]. In addition, we also monitor the landslide front position and speed U using an overhead fast camera (Phantom v641) at a frame rate of 100 Hz. To determine U we use a standard image processing tool (ImageJ) to manually track the front position of the landslide, which is easily distinguished in the experiments [see Fig. 1(b) and SM [19]]. Our grains are relatively spherical glass beads which have been roughly presorted by the manufacturer according to diameter D, ranging from ∼45 μm to ∼1.5 mm, and we characterize the size and shape distributions of the grains using an imaging technique [53] (see also SM [19]). Following typical practice in natural landslide studies, instead of the frequency distribution we use the mass-weighted distribution $p(D)$, which emphasizes large grains, to determine average quantities such as $\langle D \rangle$ and $\langle D^3 \rangle$ (see SM [19]). We observe no substantial influence of electrostatic effects on the landslide runout distance.

In Fig. 2(a) we show different experimental curves of Heim's ratio H/L versus V (we consider even lower V in the accompanying paper [51]). In our experiments we systematically vary $\langle D \rangle$ and H, and perform experiments for a large range of V. This creates a jumble of data. Varying H or $\langle D \rangle$ creates a new curve, but it is similar in shape, follows the classical trend, and is only shifted vertically. Such influence is not surprising and has been previously noted [17,49], but to our knowledge the quantitative dependence has never been elucidated. Inspired by the similarity of the individual curves and a systematic dependence on H and $\langle D \rangle$, we seek a self-similar function for the dependence of L on V, H, and D.

We find inspiration for this solution from the results of large-scale experiments of up to 550000 ping-pong balls released on a ski jump and in the laboratory [54–56]. These experiments found that the front speed U scales with the size of the system, represented by the number of ping-pong balls N, as $U \sim N^{1/6} \sim V^{1/6}$. Here we extend their analysis by determining the dependence on D and H. We found that while our laboratory experiments also roughly yield $U \sim V^{1/6}$ (see SM [19]), for proper comparison we must nondimensionalize U and V. This requires at least one length scale l (the velocity can be nondimensionalized with $\sqrt{gl}$, where g is the gravitational acceleration). We determined that U does not depend on H (see SM [19]), so we instead turn to D. Because the mobility of granular flow has

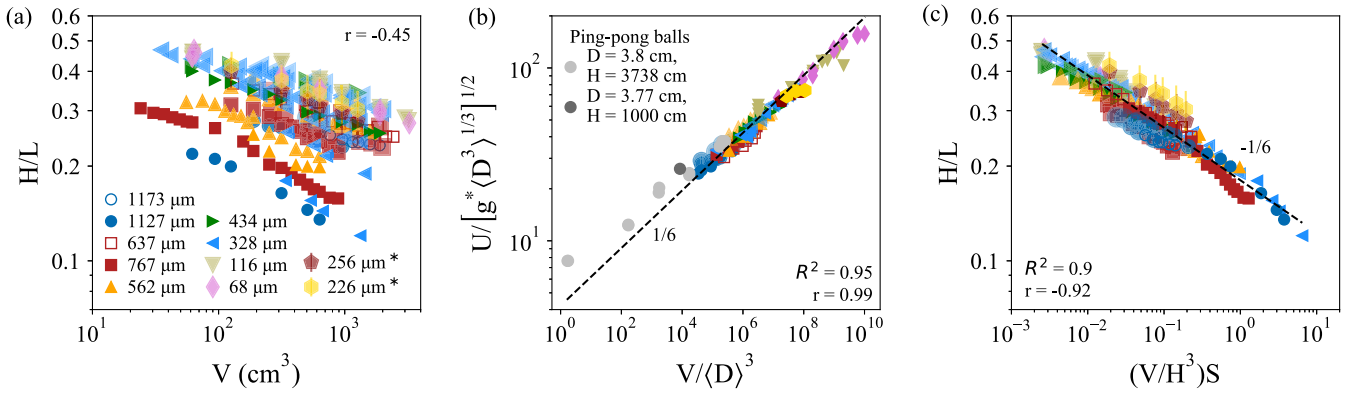

FIG. 2. Plots of runout and U from the laboratory experiments with corresponding Spearman correlation coefficients r for all data in each subplot. (a) A traditional plot of (H/L) versus V for laboratory experiments with different $\langle D\rangle$ and H ($5 \lesssim H \lesssim 37$ cm; data symbols for larger H are bigger and more transparent). An overall negative trend is in keeping with natural landslides [4], but the data show scatter and a clear dependence on D and H. Grain sizes in the legend refer to $\langle D\rangle$. The two grains marked by asterisks are bidisperse mixtures with large $S \simeq 4$. Error bars determined from repeating experiments are smaller than the data symbols except for the bidisperse grains. (b) A plot of the front speeds U versus V from experiments and ping-pong ball experiments [54–56] normalized using the grain-size distribution $(\langle D^3\rangle, \langle D\rangle)$. All dashed lines are a power-law fit with exponent $1/6$. The linear least squares best-fit exponent is 0.143 ± 0.002. (c) The runout data collapse by taking into account both D and H in the normalization and go as $H/L \sim [(V/H^3)S]^{-1/6}$ (dashed line). The linear least squares best-fit exponent is -0.156 ± 0.003.

been linked to its particle size distribution $[p(D)]$ in laboratory experiments [57], two-dimensional simulations [58], and in granular slumping experiments and simulations [59], we anticipate that U may depend on various moments of $p(D)$. We choose the first ($\langle D\rangle$) and third ($\langle D^3\rangle$) moments, the latter of which is related to the asymmetry of $p(D)$. Although important to better represent $p(D)$, using two length scales creates an ambiguity for the choice of normalization, exacerbated by the fact that in most of the laboratory and ping-pong experiments their ratio is $S \equiv \langle D^3\rangle/\langle D\rangle^3 \sim 1$. We thus perform several experiments with mixed grains to obtain more asymmetric distributions ($S \sim 4$) and find substantially better collapse when we normalize U using $\langle D^3\rangle$ and V using $\langle D\rangle$ (see SM [19]). We thus define a characteristic speed $\sqrt{g^*\langle D^3\rangle^{1/3}}$, where $g^* = g(1 - \rho_{\text{air}}/\rho)(\sin\theta - \mu_{\text{sliding}}\cos\theta)$, g is the gravitational acceleration, ρ_{air} is the air density, and μ_{sliding} is the sliding friction coefficient from the literature [60,61]. We plot the result in Fig. 2(b). Not only is the laboratory collapse improved (a fit to a $1/6$ power law changes to $R^2 \simeq 0.95$ from $R^2 \simeq 0.85$ when the data are not normalized), but the laboratory and ping-pong data are brought into close correspondence. The best-fit exponent determined using linear least squares also yields an exponent 0.143 ± 0.002 similar to the expected $1/6$ ($\simeq$0.166).

We connect this result for the motion of the landslide with its runout using a simple argument. We estimate L using the front speed U so that $L \sim UT$, where T is a characteristic time we assume to go as $T \sim \sqrt{H/g^*}$ as observed in granular slumping experiments [45]. We thus estimate Heim's ratio as $H/L = H/UT$, yielding

$$\frac{H}{L} \sim \frac{H\sqrt{g^*\langle D\rangle}}{\sqrt{Hg^*\langle D^3\rangle^{1/3}V^{1/3}}} \sim \left[\left(\frac{V}{H^3}\right)S\right]^{-1/6}, \qquad (1)$$

where only the final term $S = \langle D^3\rangle/\langle D\rangle^3$ depends on the granularity through the asymmetry of $p(D)$. We test this prediction in Fig. 2(c), in which we observe an appreciable improvement over the traditional plot in Fig. 2(a), as well as agreement with the exponent $-1/6$. Our simple argument together with Fig. 2 not only demonstrate for the first time that the quantitative dependence of the runout distance on H is through the square root ($\propto \sqrt{H}$) but that the runout speed and distance also depend on the grain distribution asymmetry through S. We found that the collapse in Figs. 2(b) and 2(c) does not hold for small values of V, with a lower limit that depends on H and D [51].

Now we apply our scaling to naturally occurring landslides, the ultimate motivation for our experiments. Unlike our relatively simple laboratory experiments, natural landslides are influenced by a host of additional parameters [13,62], some of which we cannot account for with a purely granular flow, so that we might not *a priori* expect our simple scaling to be relevant. Indeed, Fig. 3(a), a traditional plot of $\mu = H/L$ versus V, visually demonstrates the apparent irrelevance of laboratory experiments to natural landslides. Even focusing on the natural landslides only, which consist of dry debris flows [4], rock avalanches [18,63,64], snow avalanches [6], and volcanic landslides [3], we observe the large scatter which has historically encouraged separate treatment for each type of mass movement. In order to test our scaling prediction [Eq. (1)], we use previously measured grain size distributions from literature

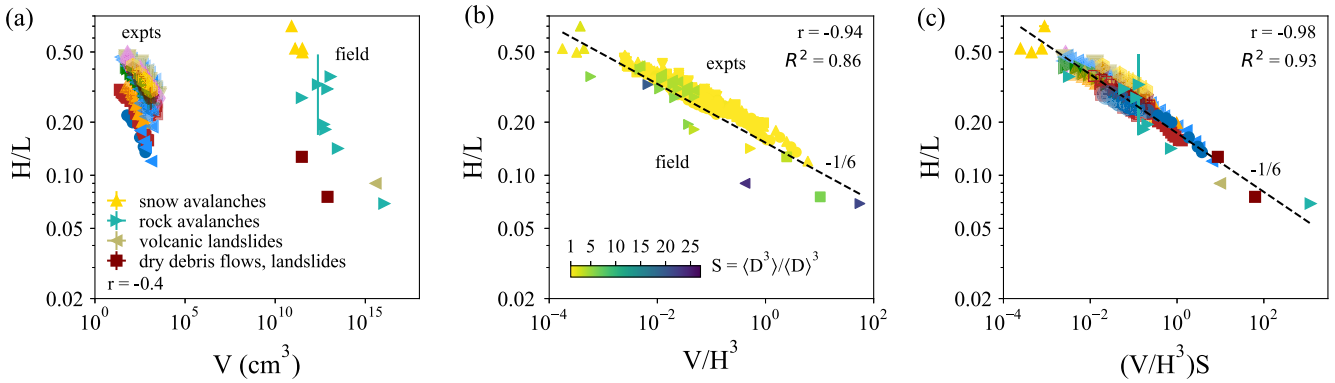

FIG. 3. Plots of runout from the laboratory, dry debris flows and landslides [4], rock avalanches [18], snow avalanches [6], volcanic landslides [3] with corresponding Spearman correlation coefficients r for all data in each subplot. We sampled laboratory data points evenly (logarithmically) spaced and with a number equal to the field data for the correlation and goodness of fit (R^2). (a) A traditional plot of H/L versus V shows large scatter and separates the field and laboratory data. (b) Replotting H/L versus V/H^3 yields a substantial improvement and reveals the dependence on $\propto H^{1/2}$. The dashed line is the predicted $-1/6$ power law. The linear least squares best-fit exponent is -0.164 ± 0.012. The values of S are indicated by the marker color with larger values tending to be below. (c) Replotting with the new scaling which includes the granularity yields excellent accord with a single, nearly universal curve $\sim[(V/H^3)S]^{-1/6}$ (dashed line). The linear least squares best-fit exponent is -0.158 ± 0.008. Error bars are determined from the spread of values for V, H, L, and D (see SM [19]).

sources, which are often extremely asymmetric, to determine S (see SM [19]).

First we consider the possible improvement from correctly accounting for H, temporarily ignoring the granularity. As Fig. 3(b) shows, when the mess of apparently distinct data [Fig. 3(a)] are plotted versus V/H^3, we observe a striking improvement in the collapse of the data, including the apparent affinity between small-scale laboratory experiments and field data which is hidden by the traditional plot [Fig. 3(a)]. Likewise, the data broadly conform to a power law with exponent $-1/6$ as predicted by our simple argument [Eq. (1)]. We thus confirm that the dependence on H through its square root is a ubiquitous feature common to landslides over a large range of drop heights, $10^0 \lesssim H \lesssim 10^5$ cm.

Next we turn to the landslide granularity. In Fig. 3(b) we have plotted the data with a color corresponding to its value of the S. While for most of the laboratory data $S \sim 1$, for the field data it can reach values of $S \sim 27$. Moreover, the data with large values of this ratio tend to fall below while those with smaller values are above. The skewness of the grain size distribution apparently increases landslide mobility, a result anticipated by two-dimensional simulations [58] and laboratory experiments [57] with grain distributions having a large bidispersity. When we include this ratio in the normalization of the system size as in Fig. 2(c) and according to Eq. (1), we find a significant improvement to the collapse of all the data, which is noticeably better than representations that exclude D (see SM [19]). In particular, including the granularity (skewness) brings the field data into even closer correspondence with the laboratory experiments.

The success of Fig. 3(c) does not signify that other factors, such as moisture [9] or topography [62], do not influence landslides. Indeed, the scatter of the data may in fact be manifestations of these other parameters. However, Fig. 3(c) suggests that it is V, H, and D which primarily determine the behavior of L. Previous work has often tried to detect the influence of other parameters using the traditional plot of H/L versus V [4,17,50], but our improved scaling now provides a framework within which to determine the role of other parameters systematically using laboratory experiments. On a practical level, the scaling result in Fig. 3(c) also provides an improved method for estimating landslide runout hazard [1]. Building on traditional methods which use historical data to predict V and H [65], with additional information about a region's associated grain size distribution, an estimate can be made of S to predict L.

In summary, we have performed an extensive experimental study of laboratory landslide runout combined with a scaling prediction that has led to a quantitative understanding of the dominant parameters that control even natural landslides. We found that the system size V, the fall height H, and the granularity D, while certainly not the only parameters, are among the most important parameters that determine the behavior of granular laboratory experiments, rock avalanches, snow avalanches, landslides, and dry debris flows. In demonstrating this we have found an impressive link between seemingly disparate systems: their granular nature.

R. T. C. gratefully acknowledges funding from the Horizon 2020 program under the Marie Skłodowska-Curie Action Individual Fellowship (MSCAIF) No. 793507, and H. K. acknowledges support from the Institut Universitaire de France. We thank Alexis Petit and Alioune Mbodji for their help in performing some of the experiments.

*rory.cerbus@riken.jp

[1] D. K. Keefer and M. C. Larsen, Assessing landslide hazards, Science **316**, 1136 (2007).

[2] S. Perkins, Death toll from landslides vastly underestimated, Nat. News **8**(2012).

[3] C. G. Newhall, Mount St. Helens, master teacher, Science **288**, 1181 (2000).

[4] F. Legros, The mobility of long-runout landslides, Eng. Geol. **63**, 301 (2002).

[5] O. Hungr, S. Leroueil, and L. Picarelli, The Varnes classification of landslide types, an update , Landslides **11**, 167 (2014).

[6] M. M. Atwater, Snow avalanches, Sci. Am. **190**, No. 1, 26 (1954).

[7] G. Magnarini, T. M. Mitchell, P. M. Grindrod, L. Goren, and H. H. Schmitt, Longitudinal ridges imparted by high-speed granular flow mechanisms in Martian landslides, Nat. Commun. **10**, 4711 (2019).

[8] R. M. Iverson and R. G. LaHusen, Dynamic pore-pressure fluctuations in rapidly shearing granular materials, Science **246**, 796 (1989).

[9] R. M. Iverson, M. Reid, N. R. Iverson, R. LaHusen, M. Logan, J. Mann, and D. Brien, Acute sensitivity of landslide rates to initial soil porosity, Science **290**, 513 (2000).

[10] T. Faug, P. Gauer, K. Lied, and M. Naaim, Overrun length of avalanches overtopping catching dams: Cross-comparison of small-scale laboratory experiments and observations from full-scale avalanches, J. Geophys. Res. Earth Surface **113**, F03009 (2008).

[11] G. S. Miller, W. Andy Take, R. P. Mulligan, and S. McDougall, Tsunamis generated by long and thin granular landslides in a large flume, J. Geophys. Res. Oceans **122**, 653 (2017).

[12] A. Daerr and S. Douady, Two types of avalanche behaviour in granular media, Nature (London) **399**, 241 (1999).

[13] R. M. Iverson, Scaling and design of landslide and debris-flow experiments, Geomorphology **244**, 9 (2015).

[14] T. Davies and M. McSaveney, Runout of dry granular avalanches, Can. Geotech. J. **36**, 313 (1999).

[15] R. Delannay, A. Valance, A. Mangeney, O. Roche, and P. Richard, Granular and particle-laden flows: From laboratory experiments to field observations, J. Phys. D **50**, 053001 (2017).

[16] A. Lucas, A. Mangeney, and J. P. Ampuero, Frictional velocity-weakening in landslides on Earth and on other planetary bodies, Nat. Commun. **5**, 3417 (2014).

[17] B. C. Johnson and C. S. Campbell, Drop height and volume control the mobility of long-runout landslides on the Earth and Mars, Geophys. Res. Lett. **44**, 12 (2017).

[18] A. Heim, *Bergsturz und Menschenleben* (Fretz & Wasmuth, Zürich, 1932), p. 20.

[19] See Supplemental Material at http://link.aps.org/supplemental/10.1103/PhysRevLett.132.254101, which includes Refs. [20–42], for additional details of the experiments and analysis.

[20] G. Bradski, The OpenCV Library, Dr. Dobb's Journal of Software Tools (2000), https://github.com/opencv/opencv/wiki/CiteOpenCV.

[21] A. Rohatgi, Webplotdigitizer (2024), https://github.com/automeris-io/WebPlotDigitizer.

[22] D. Chang, L. Zhang, Y. Xu, and R. Huang, Field testing of erodibility of two landslide dams triggered by the 12 May Wenchuan earthquake, Landslides **8**, 321 (2011).

[23] E. Getahun, S.-w. Qi, S.-f. Guo, Y. Zou, and N. Liang, Characteristics of grain size distribution and the shear strength analysis of Chenjiaba long runout coseismic landslide, J. Mt. Sci. **16**, 2110 (2019).

[24] Y. Yin, F. Wang, and P. Sun, Landslide hazards triggered by the 2008 Wenchuan earthquake, Sichuan, China, Landslides **6**, 139 (2009).

[25] G. E. Manger *et al.*, Porosity and bulk density of sedimentary rocks, Bull. U.S. Geol. Surv. **1144-E**, 1 (1963).

[26] T. Huang, M.-t. Ding, T. She, S.-j. Tian, and J.-t. Yang, Numerical simulation of a high-speed landslide in Chenjiaba, Beichuan, China, J. Mt. Sci. **14**, 2137 (2017).

[27] E. Vitz, J. W. Moore, J. Shorb, X. Prat-Resina, T. Wendorff, and A. Hahn, Density of rocks and soils (2020), [Online; accessed 2021-03-23].

[28] B. Andreotti, Y. Forterre, and O. Pouliquen, *Granular Media: Between Fluid and Solid* (Cambridge University Press, Cambridge, England, 2013).

[29] R. McGeary, Mechanical packing of spherical particles, J. Am. Ceram. Soc. **44**, 513 (1961).

[30] H. J. H. Brouwers, Particle-size distribution and packing fraction of geometric random packings, Phys. Rev. E **74**, 031309 (2006).

[31] B. Voight, R. Janda, H. Glicken, and P. Douglass, Nature and mechanics of the Mount St. Helens rockslide-avalanche of 18 May 1980, Geotechnique **33**, 243 (1983).

[32] P. Bartelt and B. W. McArdell, Granulometric investigations of snow avalanches, J. Glaciol. **55**, 829 (2009).

[33] B. Sovilla, P. Burlando, and P. Bartelt, Field experiments and numerical modeling of mass entrainment in snow avalanches, J. Geophys. Res. **111**, 10.1029/2005JF000391 (2006).

[34] M. McSaveney and T. Davies, Rockslides and their motion, in *Progress in Landslide Science* (Springer, New York, 2007), pp. 113–133.

[35] S. A. Dunning, Rock avalanches in high mountains, Ph.D. thesis, University of Bedfordshire, 2004.

[36] S. Homuth, A. Götz, and I. Sass, Reservoir characterization of the upper Jurassic geothermal target formations (Molasse Basin, Germany): Role of thermofacies as exploration tool, Geoth. Energ. Sci. **3**, 41 (2015).

[37] S. Cox and S. Allen, Vampire rock avalanches of January 2008 and 2003, Southern Alps, New Zealand, Landslides **6**, 161 (2009).

[38] M. Charrière, F. Humair, C. Froese, M. Jaboyedoff, A. Pedrazzini, and C. Longchamp, From the source area to the deposit: Collapse, fragmentation, and propagation of the Frank slide, Geol. Soc. Am. Bull. **128**, 332 (2016).

[39] W. V. Gassen and D. Cruden, Momentum transfer and friction in the debris of rock avalanches, Can. Geotech. J. **26**, 623 (1989).

[40] B. Benko and D. Stead, The Frank slide: A reexamination of the failure mechanism, Can. Geotech. J. **35**, 299 (1998).

[41] S. G. Evans, O. Hungr, and J. J. Clague, Dynamics of the 1984 rock avalanche and associated distal debris flow on Mount Cayley, British Columbia, Canada: Implications for landslide hazard assessment on dissected volcanoes, Eng. Geol. **61**, 29 (2001).

[42] D. Cruden and Z. Lu, The rockslide and debris flow from Mount Cayley, BC, in June 1984, Can. Geotech. J. **29**, 614 (1992).
[43] P. Jop, Y. Forterre, and O. Pouliquen, A constitutive law for dense granular flows, Nature (London) **441**, 727 (2006).
[44] Y. Forterre and O. Pouliquen, Flows of dense granular media, Annu. Rev. Fluid Mech. **40**, 1 (2008).
[45] E. Lajeunesse, J. Monnier, and G. Homsy, Granular slumping on a horizontal surface, Phys. Fluids **17**, 103302 (2005).
[46] M. Pirulli and A. Mangeney, Results of back-analysis of the propagation of rock avalanches as a function of the assumed rheology, Rock mechanics and rock engineering **41**, 59 (2008).
[47] S. Parez and E. Aharonov, Long runout landslides: A solution from granular mechanics, Front. Phys. **3**, 80 (2015).
[48] M. Kesseler, V. Heller, and B. Turnbull, Grain Reynolds number scale effects in dry granular slides, J. Geophys. Res. **125**, e2019JF005347 (2020).
[49] J. Fei, Y. Jie, X. Sun, and X. Chen, Particle size effects on small-scale avalanches and a μ (i) rheology-based simulation, Comput. Geotech. **126**, 103737 (2020).
[50] B. C. Johnson, C. S. Campbell, and H. J. Melosh, The reduction of friction in long runout landslides as an emergent phenomenon, J. Geophys. Res. **121**, 881 (2016).
[51] R. T. Cerbus, L. Brivady, T. Faug, and H. Kellay, companion article, Air drag controls the runout of small laboratory landslides, Phys. Rev. E **109**, 064907 (2024).
[52] A. Lucas, A. Mangeney, D. Mège, and F. Bouchut, Influence of the scar geometry on landslide dynamics and deposits: Application to Martian landslides, J. Geophys. Res **116**, 10.1029/2011JE003803 (2011).
[53] R. T. Cerbus, T. Faug, and H. Kellay, A landslide granular phase transition, EPJ Web Conf. **249**, 03003 (2021).
[54] J. McElwaine and K. Nishimura, Ping-pong ball avalanche experiments, Ann. Glaciol. **32**, 241 (2001).
[55] K. Nishimura, S. Keller, J. McElwaine, and Y. Nohguchi, Ping-pong ball avalanche at a ski jump, Granular Matter **1**, 51 (1998).
[56] K. Kosugi, A. Sato, O. Abe, Y. Nohguchi, Y. Yamada, K. Nishimura, and K. Izumi, Table tennis ball avalanche experiments, in *Proceedings of the International Snow Science Workshop (ISSW94)*, Vol. 3, pp. 636–642, https://arc.lib.montana.edu/snow-science/about.php.
[57] F. Moro, T. Faug, H. Bellot, and F. Ousset, Large mobility of dry snow avalanches: Insights from small-scale laboratory tests on granular avalanches of bidisperse materials, Cold Reg. Sci. Technol. **62**, 55 (2010).
[58] E. Linares-Guerrero, C. Goujon, and R. Zenit, Increased mobility of bidisperse granular avalanches, J. Fluid Mech. **593**, 475 (2007).
[59] Z. Lai, L. E. Vallejo, W. Zhou, G. Ma, J. M. Espitia, B. Caicedo, and X. Chang, Collapse of granular columns with fractal particle size distribution: Implications for understanding the role of small particles in granular flows, Geophys. Res. Lett. **44**, 12 (2017).
[60] T. Pongó, V. Stiga, J. Török, S. Lévay, B. Szabó, R. Stannarius, R. C. Hidalgo, and T. Börzsönyi, Flow in an hourglass: Particle friction and stiffness matter, New J. Phys. **23**, 023001 (2021).
[61] Y. Inaba, S. Tamaki, H. Ikebukuro, K. Yamada, H. Ozaki, and K. Yoshida, Effect of changing table tennis ball material from celluloid to plastic on the post-collision ball trajectory, J. Human Kinetics **55**, 29 (2017).
[62] J. Aaron and S. McDougall, Rock avalanche mobility: The role of path material, Eng. Geol. **257**, 105126 (2019).
[63] M. McSaveney, Recent rockfalls and rock avalanches in Mount Cook National Park, New Zealand, in *Catastrophic Landslides: Effects, Occurrence, and Mechanisms* (Geological Society of America, Boulder, 2002), Vol. 15, pp. 35–70.
[64] O. A. Pfiffner, The Flims rock avalanche: Structure and consequences, Swiss J. Geosci. **115**, 1 (2022).
[65] M. Cardinali, P. Reichenbach, F. Guzzetti, F. Ardizzone, G. Antonini, M. Galli, M. Cacciano, M. Castellani, and P. Salvati, A geomorphological approach to the estimation of landslide hazards and risks in Umbria, Central Italy, Nat. Hazards Earth Syst. Sci. **2**, 57 (2002).